UNPUBLISHED PRELIMINARY DATA

THE PENNSYLVANIA
STATE UNIVERSITY

IONOSPHERIC RESEARCH

Scientific Report No. 223(E)

A PROBE ASSEMBLY FOR THE DIRECT MEASUREMENT OF IONOSPHERIC PARAMETERS

by

L. C. Hale

October 20, 1964

(ACCESSION NUMBER)	(THRU)
33 (PAGES)	1 (CODE)
(NASA CR OR TMX OR AD NUMBER)	(CATEGORY)

IONOSPHERE RESEARCH LABORATORY

University Park, Pennsylvania

NASA Grant No. NsG-134-61

REPORTS CONTROL No.

Ionospheric Research

NASA Grant No. NsG-134-61

Scientific Report

on

"A Probe Assembly for the Direct Measurement of Ionospheric Parameters"

by

L. C. Hale

October 20, 1964

Scientific Report No. 223(E)

Submitted by: L. C. Hale (aw)
L. C. Hale, Assistant Professor of Electrical Engineering

Approved by: J. S. Nisbet (aw)
J. S. Nisbet, Associate Professor of Electrical Engineering

Approved by: A. H. Waynick
A. H. Waynick, Director, Ionosphere Research Laboratory

Ionosphere Research Laboratory

The Pennsylvania State University

College of Engineering

Department of Electrical Engineering

Table of Contents

33223

Abstract

A direct probe for measurement of ionospheric parameters - positive ion density, composition, and temperature, electron temperature and vehicle potential is described in detail. The probe is based on a design suggested by Bennett and Pearse. This design has been implemented by the construction of a rugged, reliable, lightweight electronics assembly with many novel and desirable features, such as simple automatic range switching of the electrometer sensitivity to both positive and negative current ranges, circuitry for extracting the time derivative of the probe current waveform, in-flight calibration of system sensitivity and automatic switching from an "ion" mode to an "electron" mode of operation.

1. Introduction

In 1957 Bennett and Pearse[1] proposed a simple method for the measurement of positive ion density in the sensible ionosphere. This method relies upon the fact that, as predicted by Jastrow and Pearse[2], the ion current to a hypersonic rocket or satellite, in most cases of interest, is determined primarily by the rate at which ions are swept out by the motion of the vehicle. A probe may be placed on the vehicle and the ion current to it can be separated from other effects by various techniques. A positive retarding potential, utilizing either a grid arrangement[3] or the collector plate potential[4,6], may be used to study the interaction energy spectrum of the ions. This energy depends, primarily, on ion mass and vehicle velocity, thus providing information on ion composition. The spectrum is "broadened" by the velocity distribution of ions, thus information on ion temperature may be obtained. Finally, since the retarding potential is the sum of the potential of the retarding grid or collector plate with respect to the spacecraft and the potential of the spacecraft, information on the spacecraft potential may be obtained using a probe of this type.

The validity of this technique has been borne out by many experiments using a number of different probe configurations[3,4,5,6]. In the case of tumbling vehicles, it is particularly convenient to use probes of spherical geometry to reduce attitude dependent effects[5,6]. For spin stabilized rocket probes and satellites or satellite platforms whose orientation is controlled to remain fixed with respect to the velocity vector of the vehicle, planar probes placed normal in the velocity vector with an unobstructed view forward into the streaming ions have performed well[3,4].

It is the purpose of this report to describe the design of such a planar probe and associated electronics which has been designed for inclusion on the Penn State - NASA "Mother-Daughter" experiment, to be launched by Argo D-4 rockets from Wallops Island, and is suitable for measurements of the ionosphere from a minimum altitude of about 100 km. to an altitude of at least several thousand kilometers. The probe described will, in addition to a rather accurate measurement of positive ion density, yield information on ion composition, ion and electron temperature, and vehicle potential.

2. Block Diagram of System

The probe and associated electronics are built into a 3" D. - 4" L. drawn aluminum can, pictured in Figure 1. The entire system, ready for flight, weighs about 1-1/2 lb. and consumes about 1/2 watt of total power.

A block diagram of the entire system is shown in Figure 2. The remainder of this report will be devoted to a description of the functions and design of the various blocks of the system, and integration of this system into the rocket and telemetry system.

3. Probe Construction

The probe geometry utilized is very close to that originally proposed by Bennett and Pearse. The assembly is pictured in Figure 3, which shows the assembly of the probe and electrometer atop the printed circuit boards comprising the associated electronics, before the electronics is potted in foam. Four tungsten grids, knitted out of 1 mil grid wire, are stretched over and welded to tungsten rings which are supported by Teflon

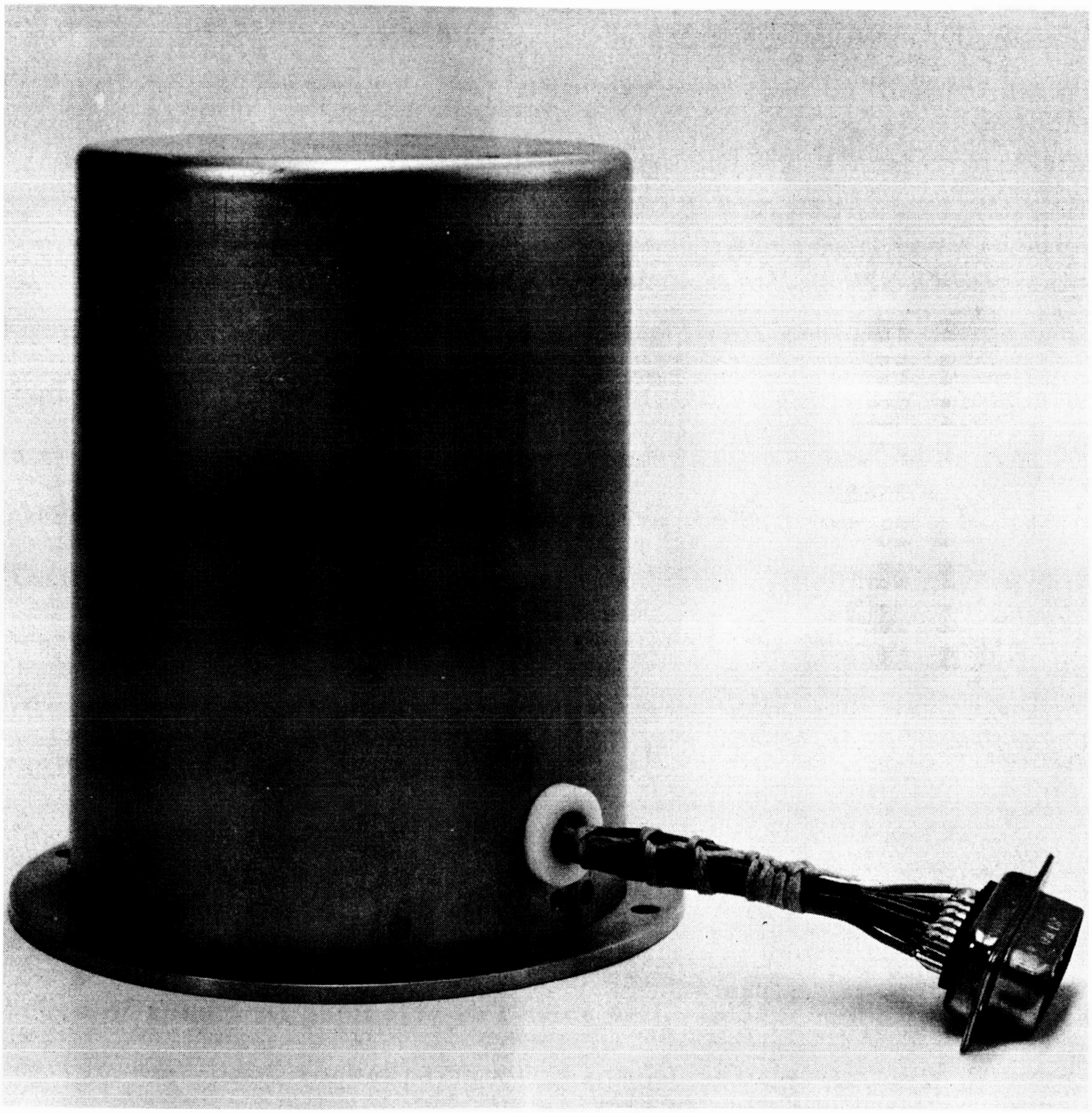

FIGURE I   COMPLETE PROBE SYSTEM

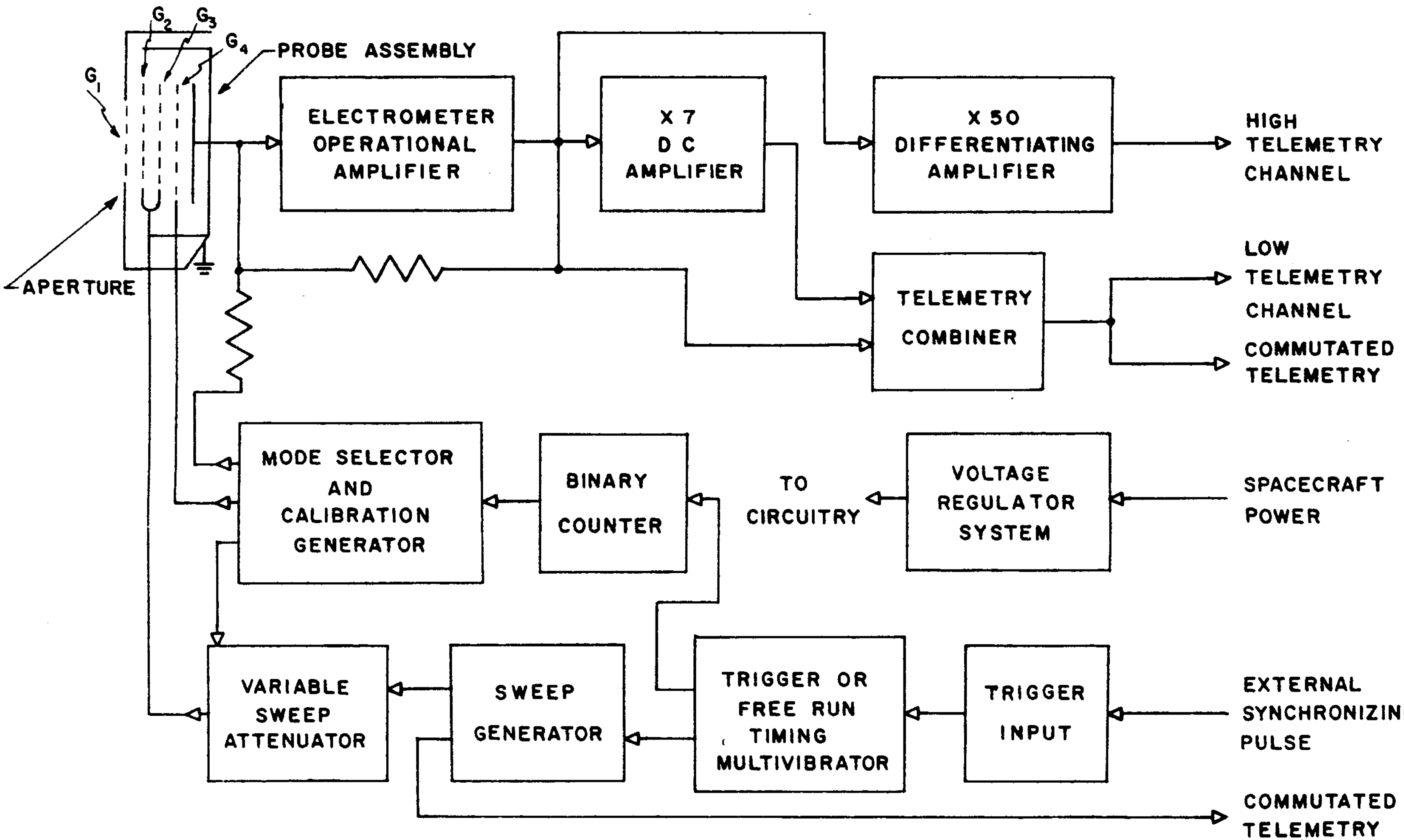

BLOCK DIAGRAM OF PROBE SYSTEM

FIGURE 2

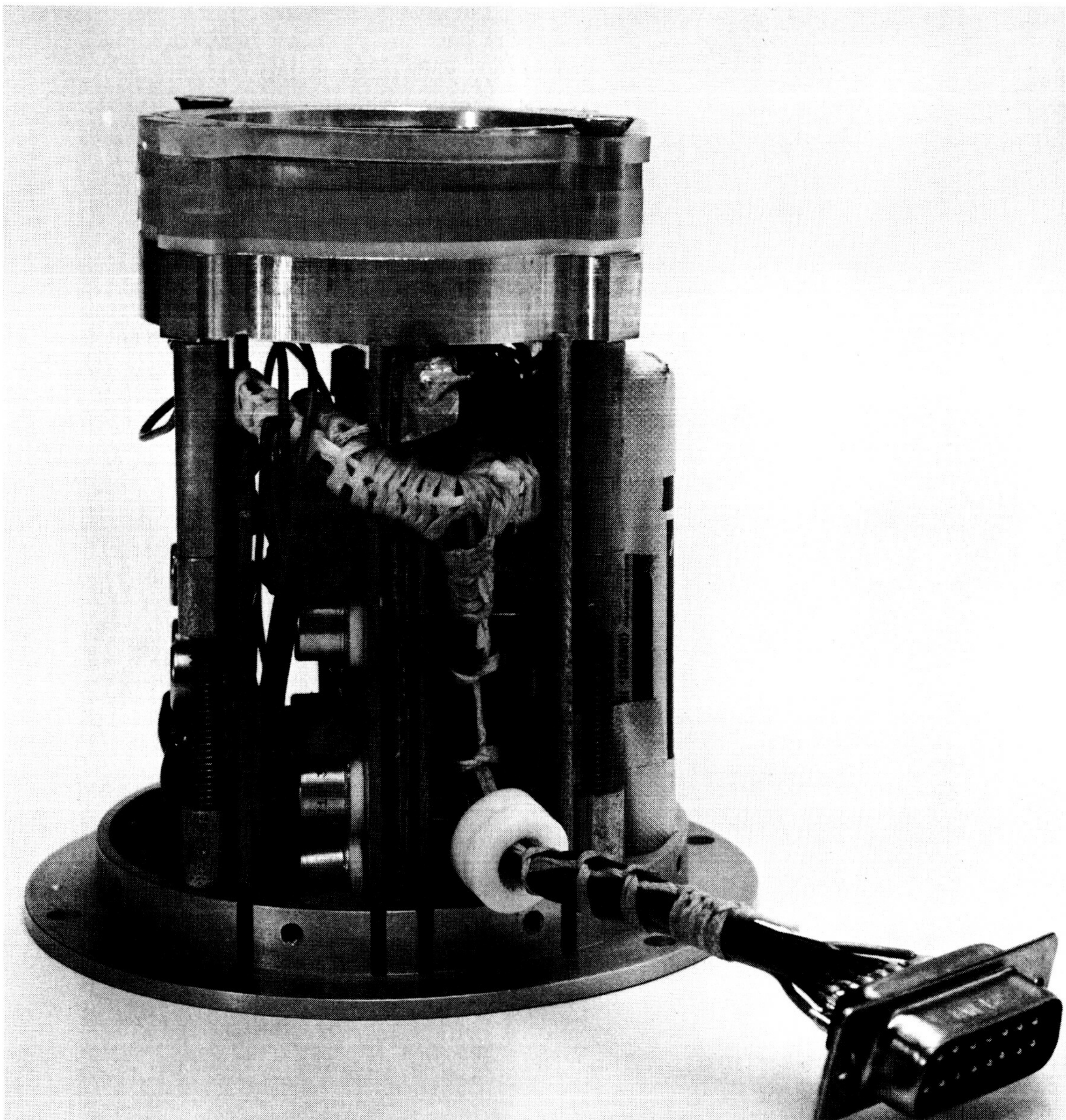

FIGURE 3 SIDE VIEW OF PROBE STRUCTURE, TOP, AND ASSORTED ELECTRONICS

or Kel-F spacer rings each 3 mm. thick. The aperture is simply a hole cut in the center of the top of the drawn aluminum housing shown in Figure 1. The aperture size may be adjusted to fit specific situations, but in any case should be appreciably smaller than the unsupported grid area, in order to reduce edge effects in the grid structure. The collector plate, also tungsten, is 1-5/8" diameter, and is riveted to a solid Teflon or Kel-F spacer.

4. Probe Operation

The probe operates alternately in an ion and electron mode, the waveforms of which are shown in Figure 4. In both modes the aperture grid G_1 is connected to the aluminum housing, which is at spacecraft potential. With respect to this potential a linear swept voltage is applied to grids G_2 and G_3, which are connected together. It is essential that a spaced double grid be used at this point in order to definitely establish a retarding potential "cage", and prevent the "tunneling" of particles that occurs when a single grid is used. In the ion mode the linear portion of the sweep voltage goes from +7 to -1.7 volts. The ion current collected in this mode will consist of those ions whose energy is sufficient to surmount the potential of grids G_2 and G_3, this energy being the sum of the kinetic interaction of the ions with the rocket and the vehicle potential. Thus as G_2 and G_3 are swept in potential, the integral energy spectrum of the ions is traced by the collector current. The sweep range used is sufficient to retard ions with the highest expected interaction energy with the Argo D-4 but would have to be increased somewhat to be useful at satellite velocities. A maximum sweep voltage

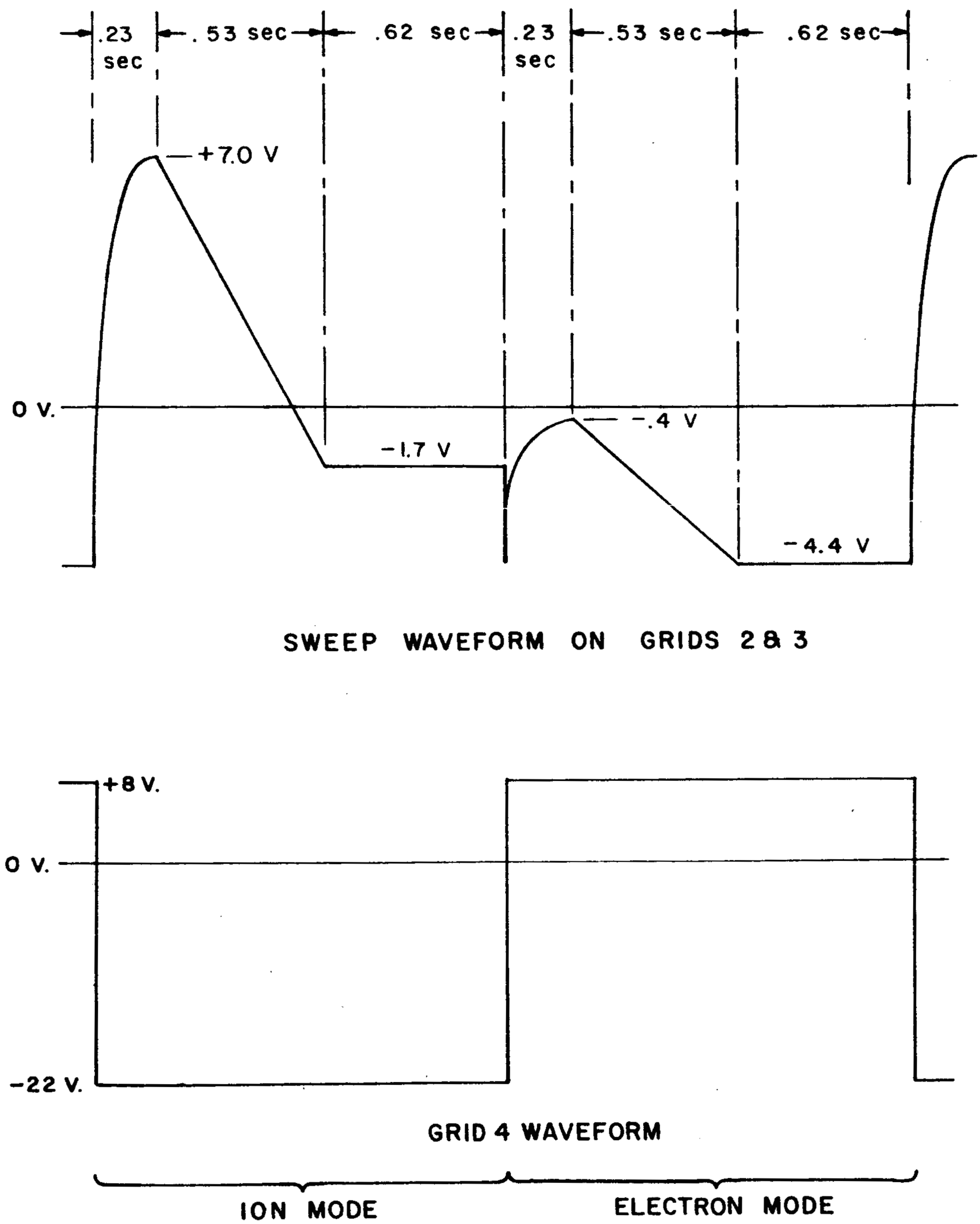

FIGURE 4 PROBE VOLTAGE WAVEFORMS

of + 15 volts would exceed the sum of spacecraft potential and maximum interaction energy with ions in all conceivable cases. On the other hand, it is desirable to use only as much sweep range as is necessary in a particular situation, in order to make maximum use of available telemetry bandwidth. During the electron mode the potential is swept linearly from -.4 to -4.4 volts. Since the spacecraft will generally acquire a small negative potential[2], only the higher energy electrons are available for measurement and determination of electron density directly is not feasible. However, the measurement of electron temperature by measuring the derivative of the probe voltage-current characteristic is a well established technique[4,6].

Grid G_3 is held at -22 volts during the ion mode, in order to suppress environmental electrons and photo-electrons from the collector plate. During the electron mode, G_3 is held at +8 volts. Since the electron temperature is determined from the derivative of the voltage-current characteristic of the probe, suppression of photo-current is not necessary in this mode of operation[4].

The collector plate is held at spacecraft potential by the use of a high-gain feedback electrometer circuit, described in the following section.

5. Electrometer Circuit

The electrometer circuit is shown in Figure 5. This basic feedback loop, designed while the writer was a Senior Visiting Fellow at University College, London, has broad application to many current measuring problems.

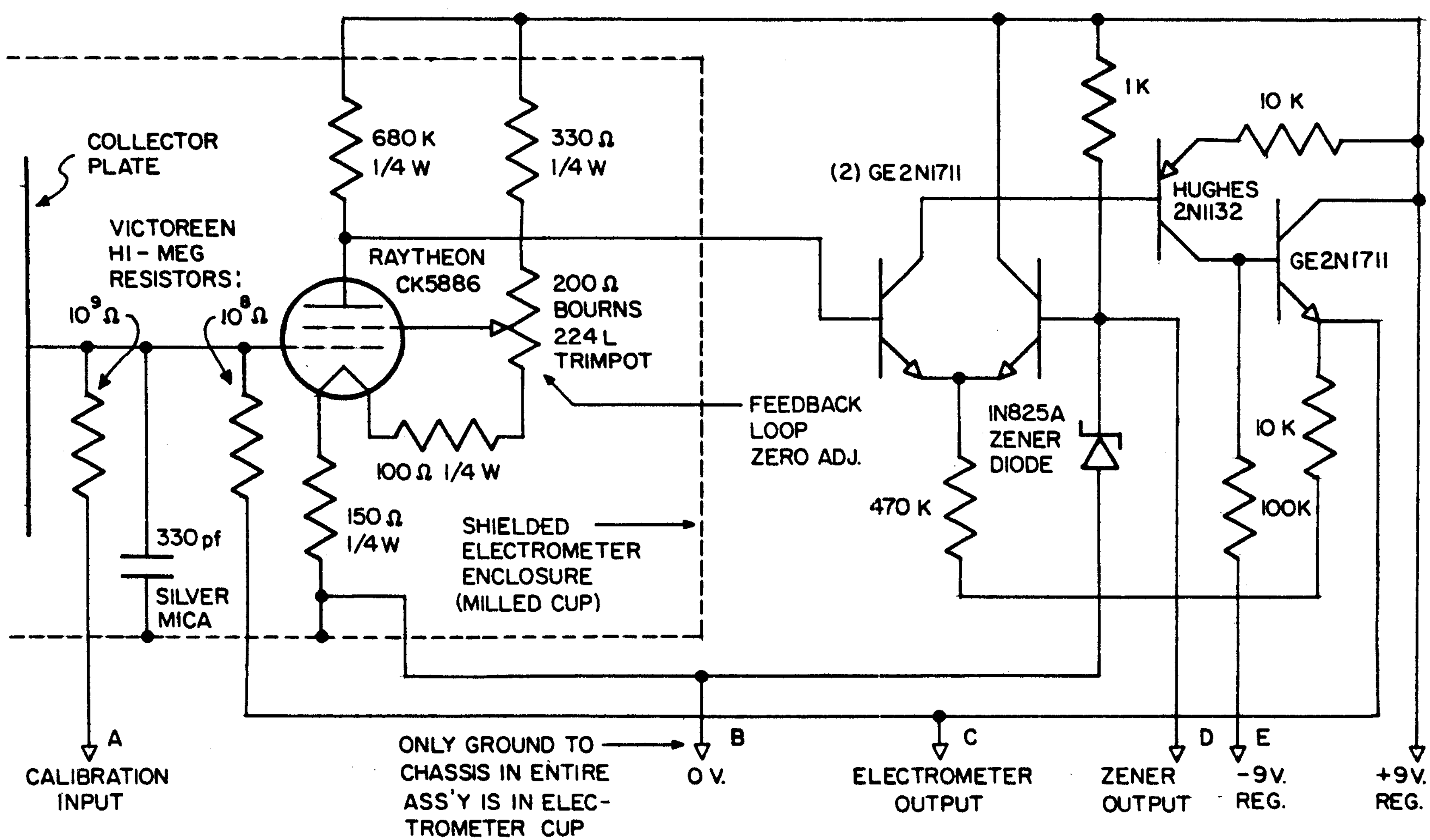

FIGURE 5 BASIC FEEDBACK ELECTROMETER CIRCUIT

The basic principle of operation is that of high gain d.c. operational amplifier with a high resistance R_F connected between the output and input terminals[7]. Ideally, the relationship of output voltage E_o to input current I_I will be :

$$E_o = -I_I R_F$$

To this must be added non-ideal effects, which may primarily be characterized by a correction term (drift) which must be added to this relationship. This correction term may, at any time, be reduced to zero by the potentiometer which controls the screen grid voltage of the CK5886 electrometer tube, and is accessible through the side of the electrometer cup, This is the only adjustment provided on the assembled experiment.

The principle cause of drift in the circuit of Figure 5 is long term drift in the characteristics of the CK5886 electrometer tube. Temperature related causes of drift can be the temperature coefficient of the zener reference diode, which is less than 100 μ V/^{o}C, and the accuracy of the differential transistor comparator, which is primarily determined by $\frac{\partial B}{\partial T}$ of transistor T_3 and can be shown to be also of the order of 100 μV/^{o}C for the component values shown[8].

In practice, long term drifts over several months, during which time prototype models have been subjected to severe environmental testing, has been less than one tenth volt, maximum, in E_o. This low drift is contingent upon aging of the electrometer tube prior to testing, by operation of the circuit continuously for about two weeks.

The action of the feedback circuit is to hold the collector plate at a very nearly constant potential, very close to that of the spacecraft. Also, the frequency response is greatly improved by the use of feedback, far beyond what is required in this application. The capacitor across the input of the electrometer circuit is used to restrict the open loop frequency response and improve the stability margin of the circuit, by providing a corner frequency much lower than others which contribute to the frequency response.

6. DC Amplifier

Because of the inherently good stability of the electrometer feedback loop, it is feasible to use a d.c. amplifier following it in order to extend the dynamic range of the current measurement and still maintain adequate stability in the output. The circuit for doing this is shown in Figure 6. This amplifier, which has been analyzed elsewhere in detail[8], has a nominal gain of seven, which is measured accurately for each probe assembly. Since the overall drift in the output of this amplifier is determined by the preceeding stages, this amplifier, which has very low drift, is more than adequate for this application.

7. Differentiating Amplifier

In order to examine more accurately the derivative of the basic probe V-I characteristic, an RC differentiator and gain of 50 d.c. amplifier are used to examine the derivative of the output of the electrometer feedback loop, as shown in Figure 6. The output of this amplifier is fed directly to one of the telemetry channels, and provides the principle information about electron temperature, ion mass, and

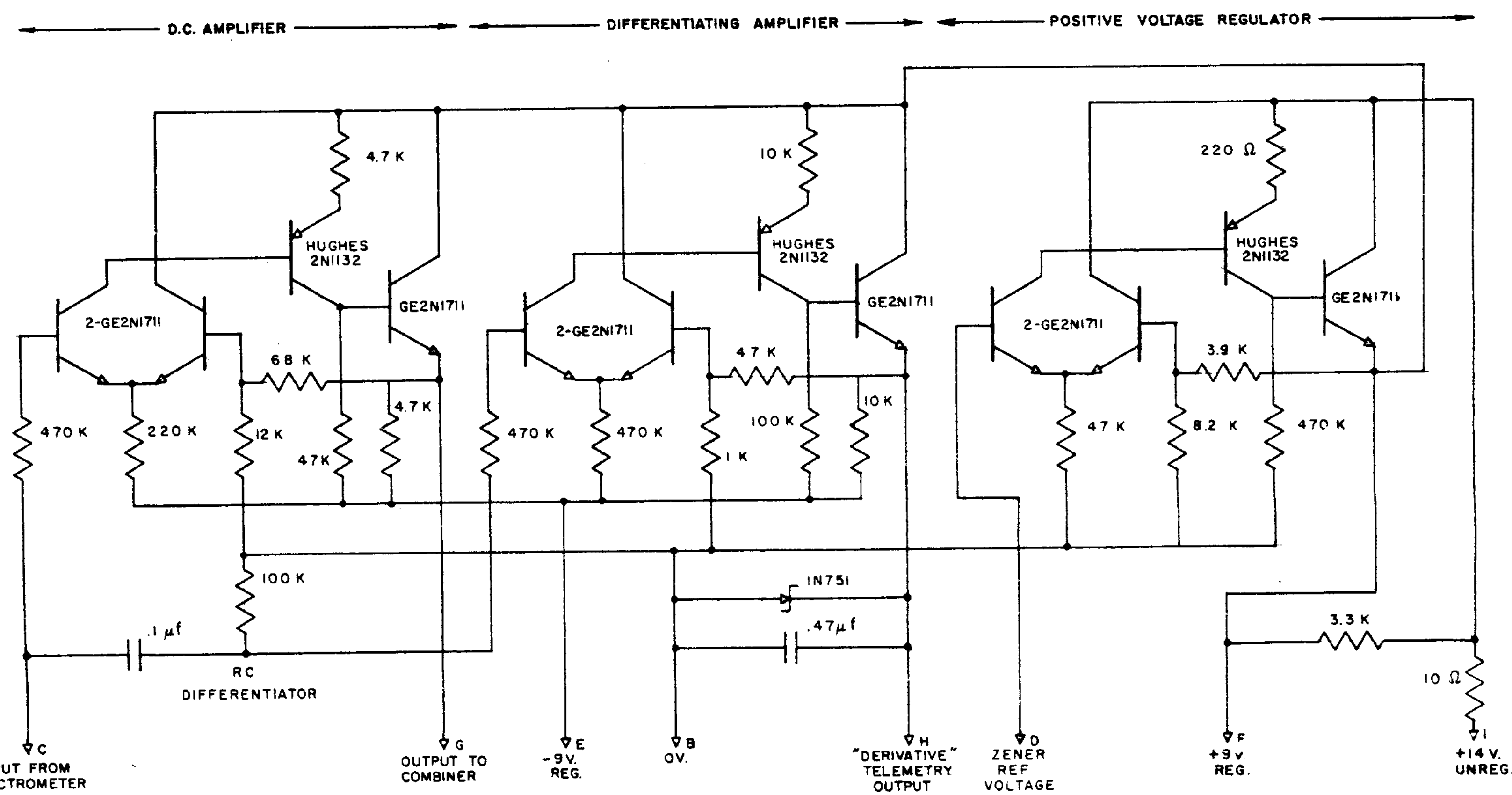

FIGURE 6 D.C. AMPLIFIER, DIFFERENTIATING AMPLIFIER, AND POSITIVE VOLTAGE REGULATOR

minor ion constituents.

8. Feedback Voltage Regulator

Also shown in Figure 6 is the voltage regulator used to power the electrometer circuitry and all other circuitry on the positive voltage line. This regulator provides one part in 10^4 regulation against large (factor of two) changes in the unregulated positive voltage input, which must not drop below 11 volts, however.

9. Amplifier Analysis

It will be noted that the electrometer operational amplifier, the d.c. amplifier, the differentiating amplifier, and the voltage regulator use the same basic four transistor circuit, with differences only in component values. This circuit is a special case of a circuit which has been analyzed elsewhere in detail[8], and the results of this analysis are summarized below for the case where the source resistance driving the input to the amplifier is relatively low ($<$ 20K), using the circuit and symbols of Figure 7:

(1) Forward Gain: The open loop forward gain is given by:

$$G_{FOL} = \frac{q\,V_1}{2kT} = 20\,V_1 \text{ at } 290^{\circ}\text{K}.$$

It will be noted that this expression is independent of transistor parameters, and since the action of the feedback loop is to hold V_1 nearly constant at the value of the negative supply voltage plus the base to emitter voltage of T_2, the open loop gain is essentially affected only by absolute temperature. This stable value of open loop gain yields a very stable closed loop forward gain, given by:

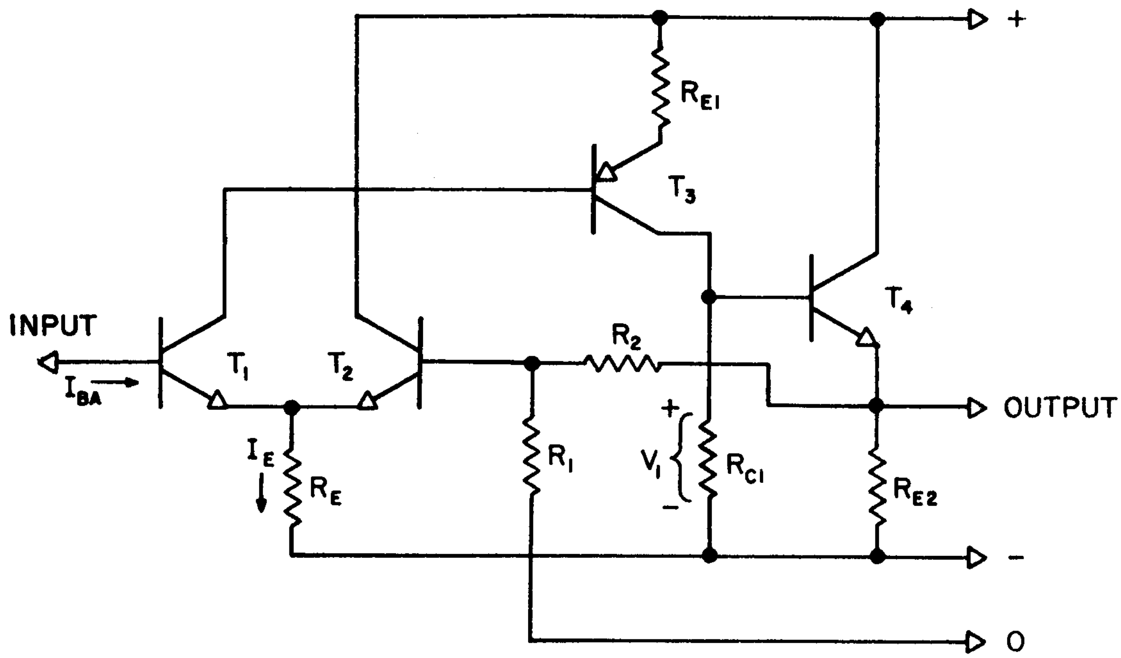

V_1: VOLTAGE ACROSS COLLECTOR RESISTOR OF T_3, R_{C1}

OTHER SYMBOLS USED IN ANALYSIS:

q : ELECTRONIC CHARGE, 1.602×10^{-19} COULOMBS

T : ABSOLUTE TEMPERATURE, °K

k : BOLTZMANN'S CONSTANT, 1.38×10^{-23} JOULES/°K

H : FEEDBACK RATIO, $\frac{R_1}{R_1 + R_2}$

$\beta_1, \beta_2, \beta_3, \beta_4$: β's OF TRANSISTOR T_1, T_2, T_3, AND T_4

FIGURE 7 BASIC AMPLIFIER CIRCUIT AND DEFINITION OF SYMBOLS

$$G_{FCL} = \frac{G_{FOL}}{1 + H\,G_{FOL}}$$

(2) Input Impedance

The product of open loop gain G_{FOL} and input impedance Z_I is given approximately by:

$$Z_I\,G_{FOL} = \beta_A\ \beta_1\ R_{C1}$$

This approximate expression is useful, since the actual input impedance will be approximately this value divided by the ratio of open loop to closed loop voltage gain, HG_{FOL}. This value will be greater than one megohm in all of the amplifiers used in this system.

The input terminal current, also an important consideration in d.c. amplifiers, is given simply by:

$$I_{BA} = \frac{I_{C1}}{\beta_1\ \ \beta_A}$$

This value will be well under one microampere for all of the amplifiers used in this system.

(3) Output impedance: The open loop output impedance will be given approximately by:

$$Z_{00L} = \frac{R_{C1}}{\beta_2}$$

This value will be divided by $H\,G_{FOL}$ to obtain the approximate closed loop output impedance.

(4) Drift rate

The drift rate of the open or closed loop transistor amplifiers, referred to the input terminals, is given by

$$D, \; V/^{\circ}C = \frac{2kT}{q} \; \frac{1}{\beta_1} \; \frac{\partial \beta_1}{\partial T}$$

Using a 2N1132 for T_1, for which $\frac{1}{\beta_1} \; \frac{\partial \beta_1}{\partial T} \approx .007$, a drift rate of about 350 $\mu V/^{\circ}C$ is obtained.

The results of the simplified analysis given above apply only in the case of low input generator impedance, and is valid for analysis of the d.c. amplifier and voltage regulator.

For the case of the electrometer differential comparator amplifier and differentiating amplifier, an expression derived for high signal source resistance must be used, and is:

$$D_H = R_{GA} \; I_{BA} \; \frac{1}{\beta_1} \; \frac{\partial \beta_1}{\partial T}$$

For typical component values in the electrometer, this will give a drift rate of about 500 $\mu V/^{\circ}C$ in the differential comparison of the zener diode voltage with the electrometer tube plate voltage. This is reduced, in calculating the drift of the overall feedback loop, by the voltage gain of the electrometer tube, which is typically about 5.

10. Amplifier Module Block

The similarity of the electrometer differential comparator amplifier, the d.c. amplifier, the differentiating amplifier, and the voltage regulator has resulted in their incorporation into a "cordwood" module block assembly, occupying a 2" x 2" space on a printed integrating board, with each individual amplifier built on a 1' x 1' printed circuit board, as pictured in Figure 7A.

11. Telemetry Combiner

In order to conserve telemetry requirements it is desirable to have an "automatic ranging" circuit which switches the lower telemetry channel to a linear scale appropriate to the magnitude and sign of the current being measured. For this purpose, a circuit has been developed which is called a telemetry combiner, and is diagrammed in Figure 8. The outputs of the electrometer and d.c. amplifier are fed into the coarse and sensitive inputs of the combiner, respectively.

The operation of the combiner is described as follows: When the d.c. amplifier output is negative, but less than about 5.5 volts in magnitude, the switching transistors TC1 and TC2 are cut-off, and the d.c. amplifier output is fed, via emitter follower TC3, level-shifting zener diode DC3, and switching diode DC4 to the telemetry output, shifted by an amount determined by the drop in DC3, DC4 and the emitter base drop in TC3, in order to appear in the standard telemetry range 0 to +5 volts. Diode DC4 provides temperature compensation for the base-emitter drop of transistor TC3 on this range, which is the most sensitive range of operation.

When the d.c. amplifier output exceeds 5.5 volts negative, the switching circuit comprising zener diode DC1 and switching transistor TC2 switches the base of emitter follower transistor TC3 to a voltage near zero and, since TC3 and TC4 form a transistor "coincidence circuit" whose output is controlled by the most negative input, the coarse input

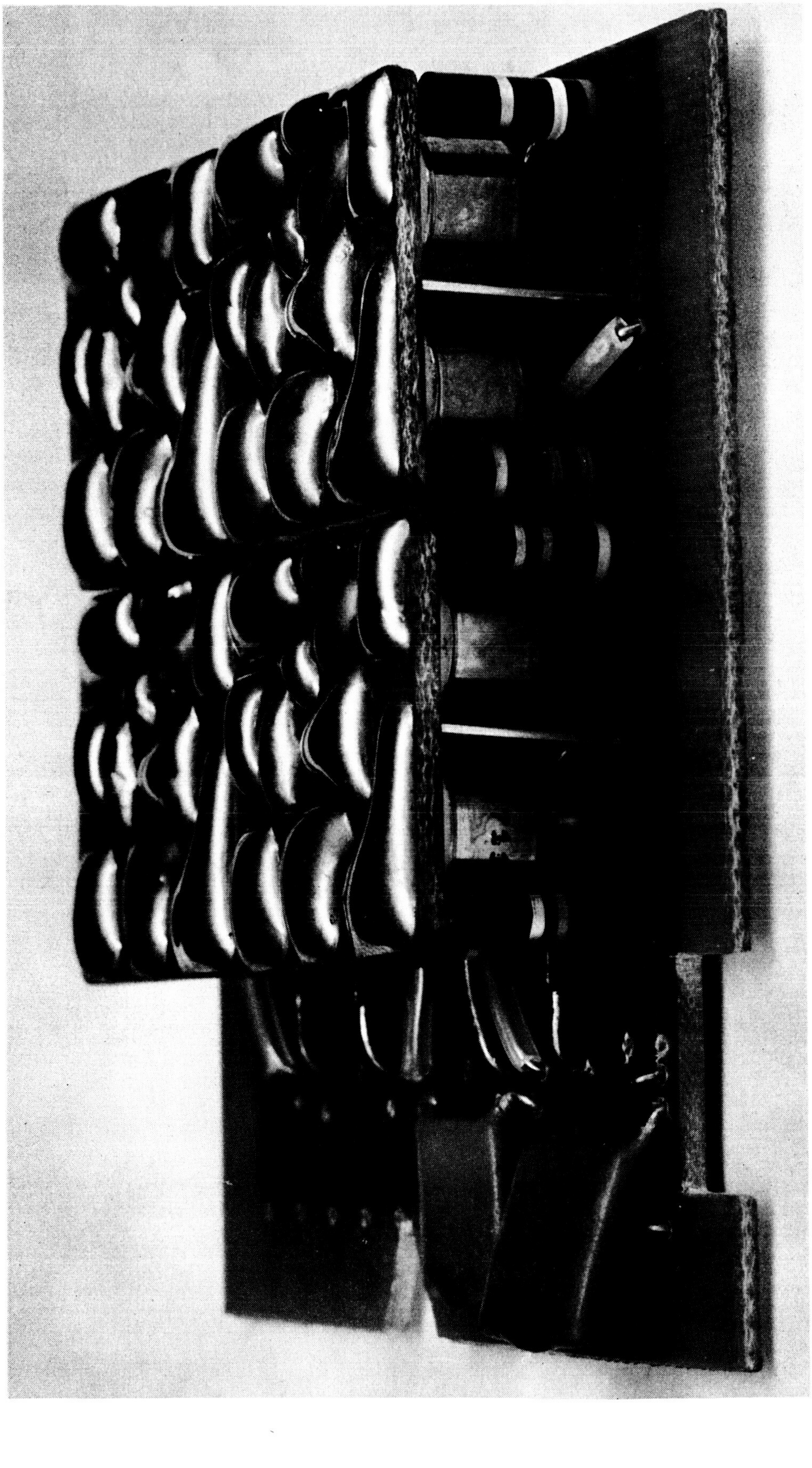

FIGURE 7A AMPLIFIER MODULE BLOCK

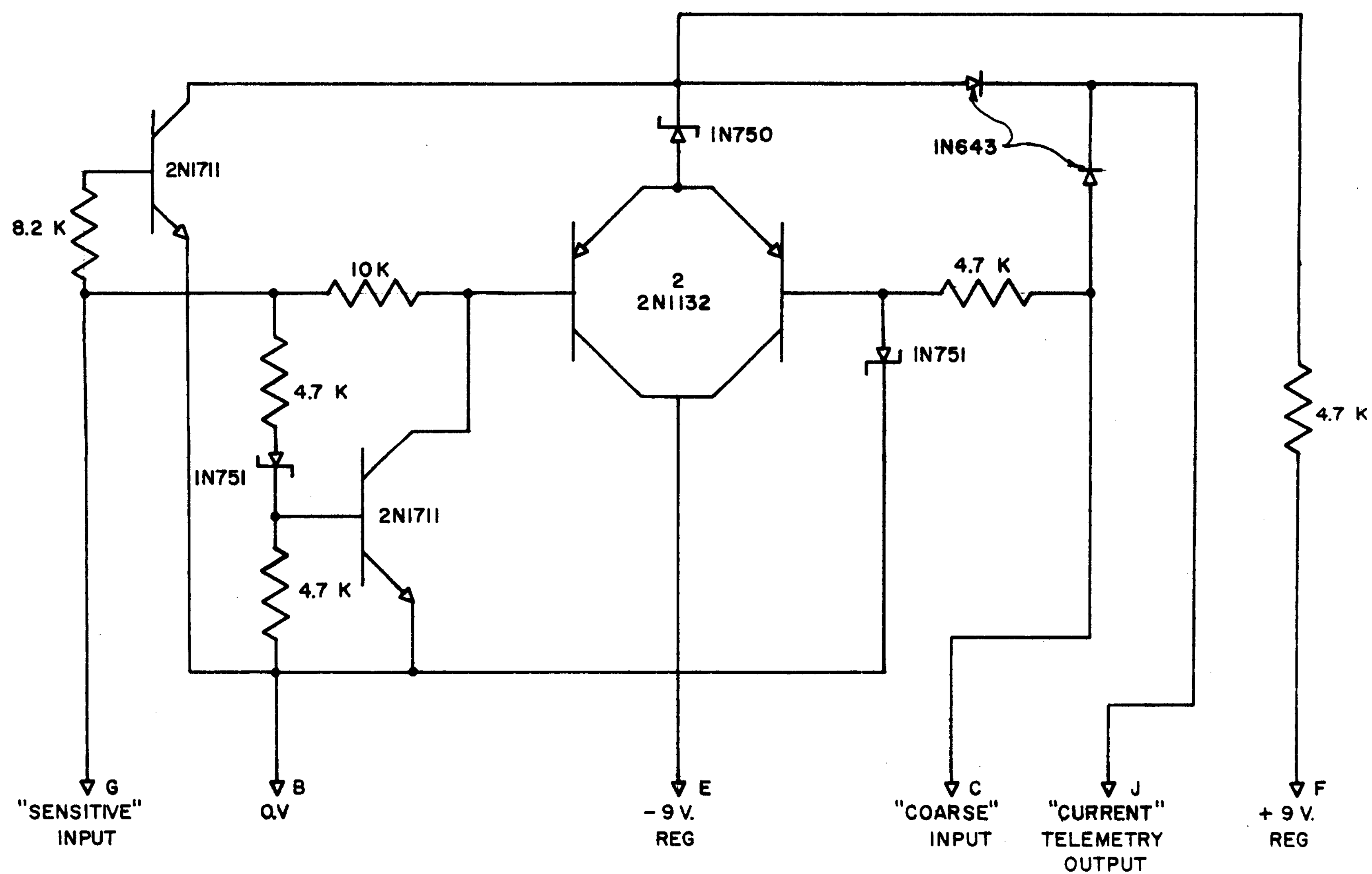

FIGURE 8 TELEMETRY COMBINER

signal from the electrometer, which is approximately .8 volts negative at the switch point, is fed via TC4, DC3, and DC4 to the output, again shifted into the 0 to +5 v. channel by the voltage drops across the base emitter terminals of TC4, and the diodes DC3 and DC4. In this mode of operation, the base-emitter drop of TC4 is temperature compensated by DC3. The zener diode DC2 limits the negative voltage on the input to TC4 to 5.1 volts, which insures that the "saturation" output of the system does not drive the telemetry out of channel. When the electrometer output goes positive, switching transistor TC1 conducts and diode DC3, operating as a switching diode, disconnects all of the circuitry heretofore described from the output, and the electrometer signal simply feeds through diode DC5 to the output, providing the "coarse" positive input range of the system.

As described above, the combiner has three ranges, sensitive and coarse for negative voltage input, and coarse for positive voltage input.

A sensitive range for "positive" voltage operation is provided via the calibration circuit of the electrometer, and consists of unbalancing the electrometer circuit with the "calibration" wavefore derived from the "mode selector" in order that the zero level for electron and ion modes of operation are shifted back and forth in the "sensitive" ragne of the combiner to utilize most of this sensitive range in both the electron and ion mode of operation, thus effectively providing four automatically switched ranges.

In subsequent work of the writer, this four range system has been extended, using similar principles, to a six range system with little added difficulty.

12. Trigger Amplifier, Timing Multivibrator, Sweep Generator

These circuits are shown in Figure 9. A stable multivibrator

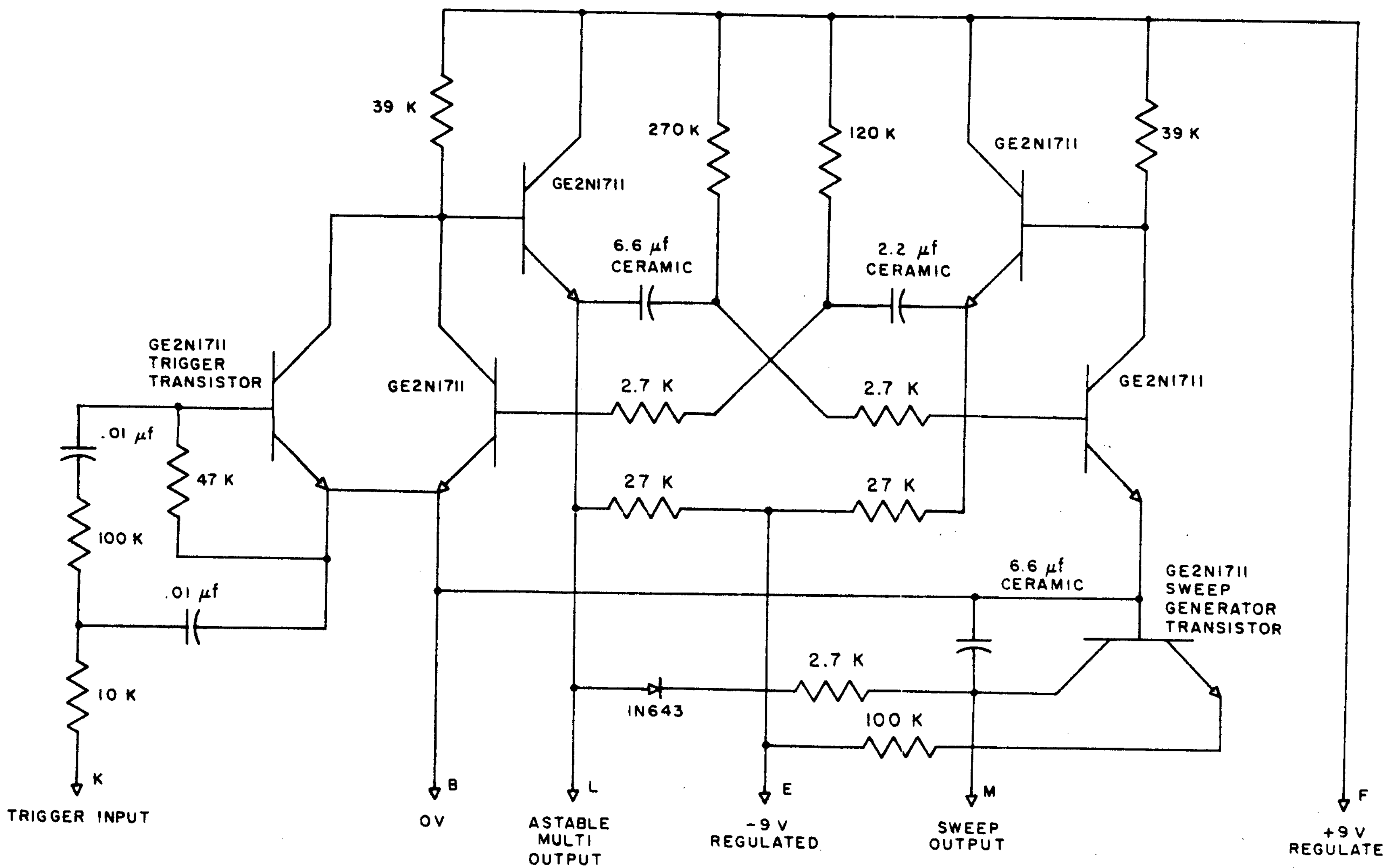

FIGURE 9 TRIGGERED ASTABLE MULTIVIBRATOR AND SWEEP GENERATOR

generates an assymetrical output which switches clearly from the full power supply voltage to zero, repetitive approximately every 1.4 seconds. During the shorter portion of the cycle, which is about .23 sec., the 6.6 μf capacitor in the sweep generator is charged to nearly the full power supply voltage through the low leakage 1N643 diode. During the long portion of the cycle, the sweep generator transistor provides a constant current discharge which provides a sweep approximately .53 sec. long, of very good linearity, going from nearly the full positive power supply voltage to a few tenths of a volt negative.

An interesting feature of this circuit is that it may be triggered at the beginning of the cycle described above in order to operate synchronously with a spacecraft timing system. The only requirement is that the triggering signal have a slightly shorter period than that of the multivibrator. If this trigger fails, the sweep generator system will continue to operate asynchronously. (Because of the danger of noise pickup on the trigger line, and the fact that no particular advantage was to be obtained from synchronous operation of the system in this particular experiment, the trigger has been disconnected in flight models of the Mother-Daughter experiment.)

13. Assembly of Combiner, Trigger Amplifier, Timing Multivibrator, and Sweep Generator

These circuits are assembled on a conventional printed circuit board as pictured in Figure 10.

14. Mode Selection and Calibration Circuitry

These circuits are shown in Figure 11, and have the function of changing the operation of the probe from the electron to ion mode on

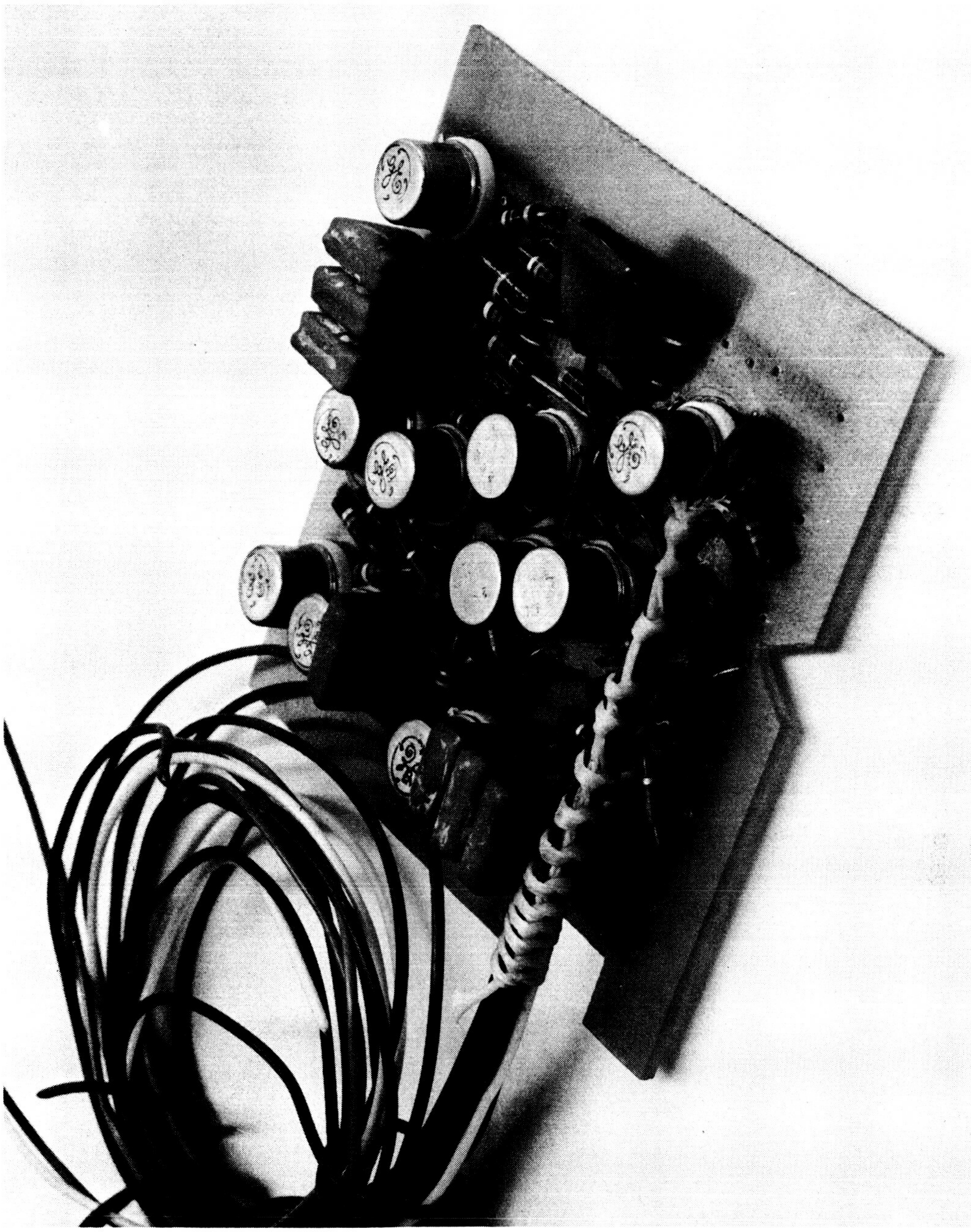

FIGURE 10 ASSEMBLY OF VARIOUS CIRCUITS

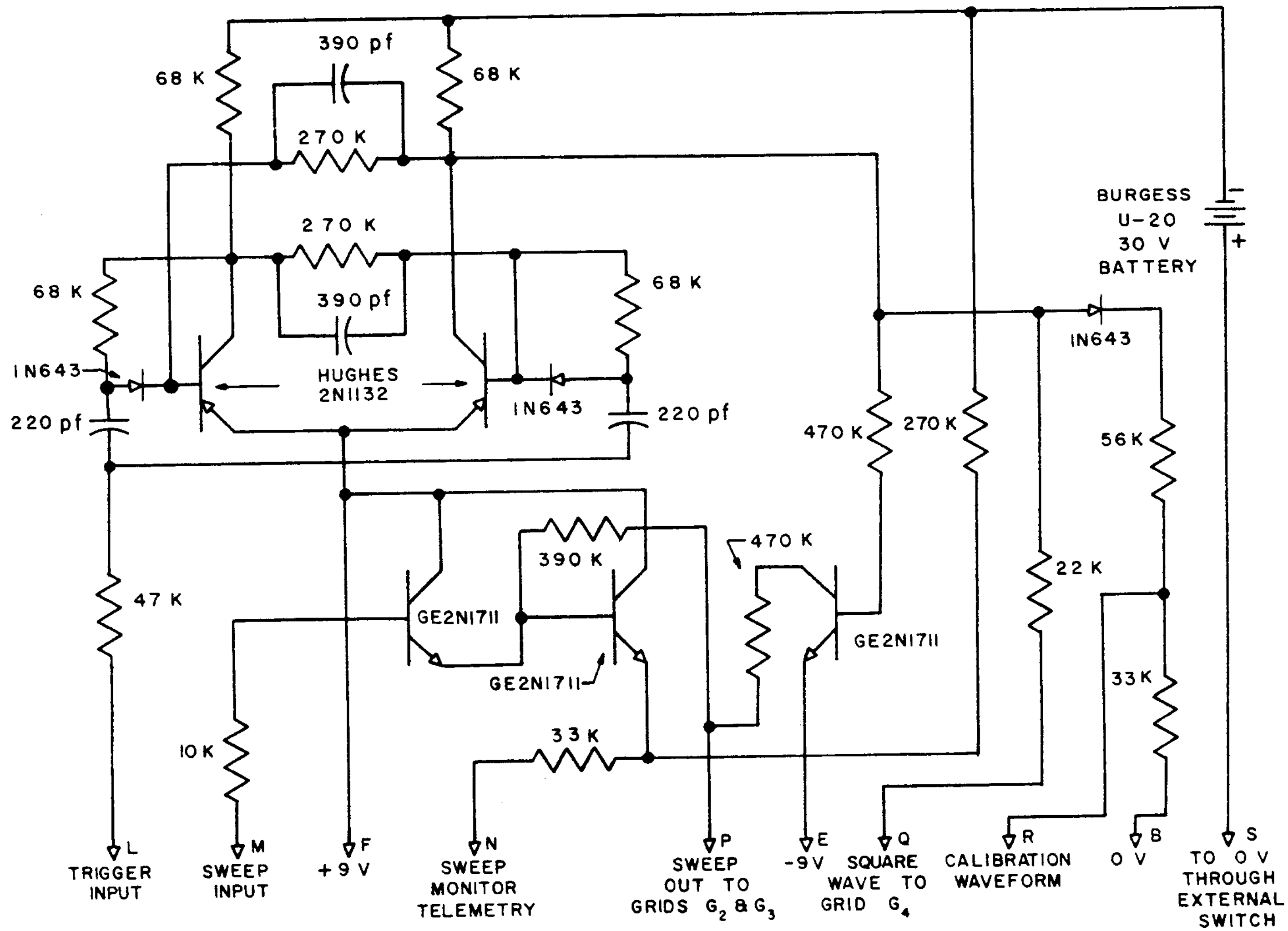

FIGURE 11 MODE SELECTOR AND CALIBRATION CIRCUITRY

alternate sweeps, and of providing an in flight calibration of the electrometer circuitry.

The binary counter is triggered by the leading edge of the timing multivibrator output which is used to generate the sweep. Since the sweep is initiated by the trailing edge of this waveform, the circuits have the "charging" portion of the timing multivibrator waveform in which to perform the changeover of function and recover from transient disturbances. The square wave generated at the collector of one of the binary transistors is used to perform the changeover. In the "on" condition this collector is at -22 volts, and in the "off" condition it is at +8 volts. This waveform is fed via a 22K resistor to grid G_4 in the probe assembly, to perform the functions described in Probe Operation. Also this waveform is fed via a diode and attenuator network to give a voltage of +3 during the "on" condition and 0 during the "off" condition. This voltage is fed to the calibration input of the electrometer, and is used to shift the balance point of the electrometer circuit between the ion and electron modes. This serves two functions. One is to provide a known shift in the telemetry output which serves as a sensitivity calibration of the entire system, including the telemetry link. The other function is to shift the output of the d.c. amplifier such as to effectively provide an additional range in the automatic range switching function provided by the telemetry combiner.

A third function of the binary waveform is to actuate the "sweep attenuator". The output of the sweep generator is fed via a Darlington pair to a commutated telemetry channel or channels, which provides a sampled record of the sweep waveform. The output of the input transistor of the Darlington pair is fed via an attenuator to grids G_2 and G_3. The attenuation of this attenuator is controlled by a transistor which is switched by the binary output, in such a manner as to produce the sweep waveform of Figure 4.

15. Integration with the Spacecraft

The integration of the probe circuitry with the spacecraft telemetry, power, and control circuitry is shown in the diagrams of Figure 12, which shows the wiring of the connectors on the probe, and on the spacecraft.

Most of the labeling in this diagram is self explanatory, but the following is added for clarification:

(1) The +14.4 (Pin 1) and -14.4 (Pin 3) volt lines should be not more than 12 and not less than 20 volts in magnitude for proper operation of the probe. Current drains of these lines are approximately 30 and 15 ma., respectively.

(2) The sweep monitor (Pins 7, 8, 9, 10) is a reproduction of the sweep waveform, primarily to provide a time reference and to check operation of the sweep generator circuitry, before the variable sweep attenuator. Attenuation of this waveform is provided so that it will fall within a standard 0 to +5 volt telemetry channel input. The exact amplitude will depend on the input resistance of the commutated telemetry channel.

(3) The "current" telemetry output (Pins 5 and 11) is the output of the automatic range switching "telemetry combiner", and the "derivative" telemetry output (Pin 6) is the output of the X50 differentiating amplifier. Frequency response requirements

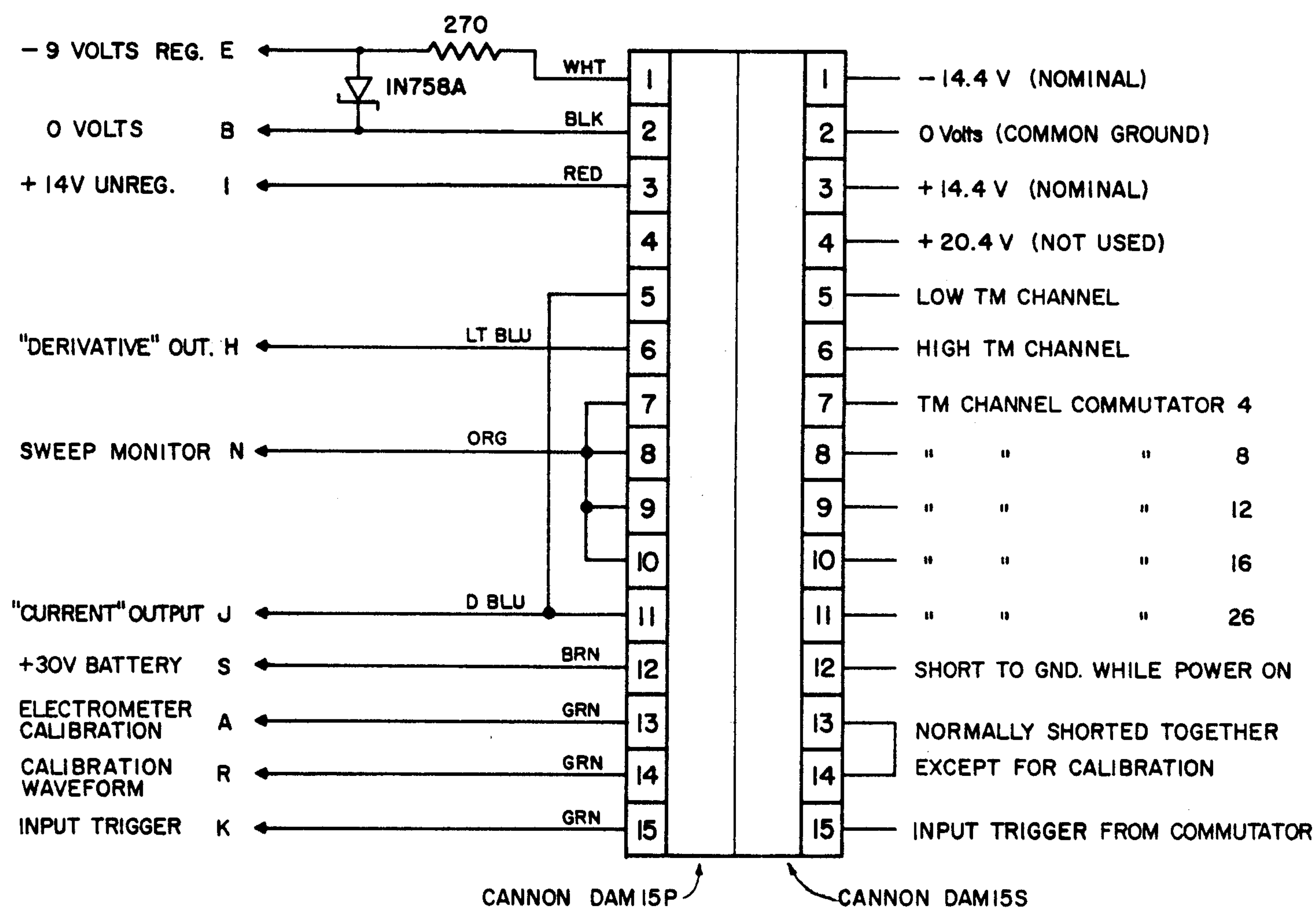

FIGURE 12 INTERFACE CONNECTIONS WITH SPACECRAFT

are of the order of one kilocycle maximum, with the higher frequency response channel going to the "derivative" channel. To provide some redundancy, the "current" telemetry is sampled on a commutated channel.

(4) The drain from the 30 volt battery, contained in the probe assembly, is less than one milliampere. This current (Pin 12) is switched to 0 v. in the spacecraft when power is turned on. <u>It must not be left on when the probe is not in use.</u>

(5) Overall calibration of the probe current sensitivity is performed by connecting a variable d.c. voltage to the "electrometer calibration" (Pin 13) input while disconnecting the jumper between Pins 13 and 14 of the spacecraft connector, or by a test set designed for this purpose. The calibration current is then given by this voltage divided by the calibration resistor built into the electrometer cup, which is $10^9\,\Omega$, ±2%. This voltage should be varied from about -70 to +70 volts to trace out the three basic ranges of the output of the telemetry combiner, measured at Pins 5 or 11.

(6) The input trigger (Pin 15) is for synchronizing the operation of the probe with the spacecraft timing circuitry. A negative pulse of fairly rapid (order of 1 millisecond) rise time and several volts amplitude (or the similar "falling" edge of a square wave), repeated at an interval of .9 to 1.3 seconds, may be used to accomplish this. (Because of the possibility of noise pickup, and the decision that asynchronous operation was preferable in this particular case, this input line has been disconnected in the "Mother-Daughter" models of this probe).

References

1. Bennett, W. H. and C. A. Pearse, Private Communication.

2. Jastrow, R., and C. A. Pearse, Atmospheric Drag on the Satellite, J. Geophys. Res., 62, 413, 1957.

3. Hanson, W. B. and D. D. McKibben, An Ion Trap Measurement of the Ion Concentration Above the F_2 Peak, J. Geophys. Res., 66, 1667, 1961.

4. Bourdeau, R. E., Donley, J. L., Whipple, E. C., and S. J. Bauer, Experimental Evidence for the Presence of Helium Ions Based on the Explorer VIII Satellite Data, J. Geophys. Res., 68, 467, 1962.

5. Boyd, R. L. F., Plasma Probes on Space Vehicles, Proceedings of the Fifth International Conference on Ionization Phenomena in Gases, August-Sept. 1961, North Holland Publishing Co., Amsterdam, 1962, pp. 1387-1397.

6. Sagalyn, R. C., Smiddy, M., and J. Wisnice, Measurement and Interpretation of Ion Density Distributions in the Daytime F Region, J. Geophys. Res., 68(1), 199, 1963.

7. Praglin, J. and W. A. Nichols, High Speed Electrometers for Rocket and Satellite Experiments, Proc. of the I. R. E., 48, 771, 1960.

8. Wilk, C. K., An Analysis of a D. C. Feedback Amplifier Suitable for Rocket Probe Instrumentation, Ionosphere Research Laboratory, Pennsylvania State University, Sci. Rept. No. 203(E).